Expanding the Molecular Spectrum of Secretory Carcinoma of Salivary Glands With a Novel *VIM-RET* Fusion

Alena Skálová, MD, PhD,† Martina Banečkova, MD,*† Lester D.R. Thompson, MD,‡ Nikola Ptáková, MSc,§ Todd M. Stevens, MD,|| Luka Brcic, MD, PhD,¶ Martin Hyrcza, MD, PhD,# Michael Michal Jr, MD, PhD,*†** Roderick H.W. Simpson, MD,# Thalita Santana, DDS, MSc,†† Michal Michal, MD,* Tomas Vaněček, PhD,§ and Ilmo Leivo, MD, PhD‡‡*

Background: Secretory carcinoma (SC), originally described as mammary analogue SC, is a predominantly low-grade salivary gland neoplasm characterized by a recurrent t(12;15)(p13;q25) translocation, resulting in *ETV6-NTRK3* gene fusion. Recently, alternative *ETV6-RET*, *ETV6-MAML3*, and *ETV6-MET* fusions have been found in a subset of SCs lacking the classic *ETV6-NTRK3* fusion transcript, but still harboring *ETV6* gene rearrangements.

Design: Forty-nine cases of SC revealing typical histomorphology and immunoprofile were analyzed by next-generation sequencing using the FusionPlex Solid Tumor kit (ArcherDX). All 49 cases of SC were also tested for *ETV6*, *RET*, and *NTRK3* break by fluorescence in situ hybridization and for the common *ETV6-NTRK3* fusions using reverse transcription polymerase chain reaction.

Results: Of the 49 cases studied, 37 (76%) occurred in the parotid gland, 7 (14%) in the submandibular gland, 2 (4%) in the minor salivary glands, and 1 (2%) each in the nasal mucosa, facial skin, and thyroid gland. SCs were diagnosed more frequently in males (27/49 cases; 55%). Patients' age at diagnosis varied from 15 to 80 years, with a mean age of 49.9 years. By molecular analysis, 40 cases (82%) presented the classic *ETV6-NTRK3* fusion, whereas 9 cases (18%) revealed an alternate fusion. Of the 9 cases negative for the *ETV6-NTRK3* fusion, 8 cases presented with *ETV6-RET* fusion. In the 1 remaining case in the parotid gland, next-generation sequencing analysis identified a novel *VIM-RET* fusion transcript. In addition, the analysis indicated that 1 recurrent high-grade case in the submandibular gland was positive for both *ETV6-NTRK3* and *MYB-SMR3B* fusion transcripts.

Conclusions: A novel finding in our study was the discovery of a *VIM-RET* fusion in 1 patient with SC of the parotid gland who could possibly benefit from *RET*-targeted therapy. In addition, 1 recurrent high-grade case was shown to harbor 2 different fusions, namely, *ETV6-NTRK3* and *MYB-SMR3B*. The expanded molecular spectrum provides a novel insight into SC oncogenesis and carries important implications for molecular diagnostics, as this is the first SC-associated translocation with a non-*ETV6* 5′ fusion partner. This finding further expands the definition of SC while carrying implications for selecting the appropriate targeted therapy.

Key Words: mammary analogue secretory carcinoma, pathology, molecular, salivary gland neoplasms, carcinoma, gene rearrangement, gene fusion, *VIM-RET*, *ETV6-NTRK3*, *ETV6-RET*

(*Am J Surg Pathol* 2020;44:1295–1307)

From the *Department of Pathology; **Biomedical Center, Faculty of Medicine in Plzen, Charles University; †Biopticka Laboratory Ltd; §Molecular Genetic Laboratory, Biopticka Laboratory Ltd, Plzen, Czech Republic; ‡Department of Pathology, Southern California Permanente Medical Group, Woodland Hills, CA; ||Department of Pathology, University of Alabama at Birmingham, Birmingham, AL; ¶Diagnostic and Research Institute of Pathology, Medical University of Graz, Graz, Austria; #Department of Pathology and Laboratory Medicine, University of Calgary, Calgary Laboratory Services, Foothills Medical Centre, Calgary, AB, Canada; ††Department of Oral Pathology, Faculty of Dentistry, University of São Paulo, São Paulo, Brazil; and ‡‡Institute of Biomedicine, Pathology, University of Turku, Turku, Finland.

Preliminary results reported as a poster presentation at the United States and Canadian Academy of Pathology Annual Meeting in National Harbor, MD, March 16-21, 2019 (Poster #411).

Conflicts of Interest and Source of Funding: The authors have disclosed that they have no significant relationships with, or financial interest in, any commercial companies pertaining to this article.

Correspondence: Alena Skálová, MD, PhD, Sikl's Department of Pathology, Charles University, Faculty of Medicine in Pilsen, E. Benese 13, Pilsen 305 99, Czech Republic (e-mail: skalova@fnplzen.cz).

Secretory carcinoma (SC), originally described as mammary analogue secretory carcinoma (MASC), is a predominantly low-grade salivary gland neoplasm characterized by a recurrent t(12;15)(p13;q25) translocation, resulting in *ETV6-NTRK3* gene fusion.[1] The same *ETV6-NTRK3* fusion gene has been recognized earlier in SC of the breast,[2] and several other rare malignancies, including infantile fibrosarcoma,[3] congenital mesoblastic nephroma,[4] papillary thyroid cancer,[5] and various hematological neoplasms.[6]

On the basis of overlapping morphologic, immunohistochemical (S100 protein and mammaglobin [MMG] positivity/p63 negativity), and molecular genetic features with SC of the breast,[2] we proposed the term "mammary analogue secretory carcinoma of salivary gland."[1] More recently, the World Health Organization (WHO) Classification of Tumors of the Head and Neck recommended a nomenclature change of MASC to SC.[7]

Since its initial description, a number of published series have expanded and further defined the clinicopathologic characteristics of salivary SC.[8–15] Histomorphologically, most tumors have been described as infiltrative. Fibrous septae divide the tumors into multiple lobules that contain microcystic/cribriform, solid, tubular/glandular, follicular, or papillary-cystic structures with abundant intraluminal secretions. The neoplastic cells appear bland with round to oval and hyperchromatic to vesicular nuclei with inconspicuous small nucleoli. The cytoplasm has an eosinophilic, granular to vacuolated appearance.[1] The recent description of 15 cases of macrocystic SC[16] further expanded the morphologic spectrum of salivary SC. Moreover, since its initial description in the salivary glands, cases of SC have been reported in a multitude of new locations, such as the skin,[17–19] the sinonasal tract,[20–22] the thyroid,[23–25] and the lung,[26] further highlighting the anatomic spectrum of this entity.

The vast majority of SC cases harbor the canonical *ETV6-NTRK3* translocation.[1] Moreover, the current WHO Classification of Tumors of the Head and Neck of 2017 recognizes that the integration of molecular advances into clinical practice is inevitable and includes the *ETV6-NTRK3* gene fusion in the definition of SC.[7] However, a subset of SC cases have been described that harbor *ETV6* gene rearrangements, but lack the classic *NTRK3* fusion partner.[27,28] With the advent of targeted next-generation sequencing (NGS) assays, this was followed by the identification of novel alternative *ETV6* partners in a subset of SCs, such as *RET*,[29] *MET*,[30] and *MAML3*.[31]

To our knowledge, this is the first *VIM-RET* gene fusion reported in SC. This finding further expands the molecular definition of SC and carries implications for diagnostics and selection of appropriate targeted therapy.

MATERIALS AND METHODS

Case Selection and Clinicopathologic Review

The study was approved by the institutional review board. Forty-eight cases of SC of salivary glands and 1 SC of thyroid gland were retrieved from routine surgical pathology files and from tumors contributed by the coauthors to the consultation files of the Salivary Gland Tumor Registry, at the Department of Pathology, Faculty of Medicine in Plzen, and Biopticka Laboratory Ltd (Plzen, Czech Republic). The cases were submitted either for confirmation of the original diagnosis or because of possible targeted treatment of the patient. Clinical follow-up was obtained from the patients, their physicians, or from referring pathologists. The histopathologic features and the immunohistochemical stains of all tumors were reviewed (A.S., M.B.), and the diagnosis of SC was confirmed on the basis of morphologic and immunohistochemical features consistent with the original description.[1] The latter features comprised coexpression of S100 protein, SOX10, CK7, and MMG in the absence of DOG1 and p63 staining.

For immunohistochemical studies, 4-μm-thick sections were cut from paraffin blocks and mounted on positively charged slides (TOMO; Matsunami Glass Inc., Japan). Sections were processed on a BenchMark ULTRA (Ventana Medical Systems, Tucson, AZ), deparaffinized, and then subjected to heat-induced epitope retrieval by immersion in a CC1 solution at pH 8.6 at 95°C. After antigen retrieval, sections were stained with a pan-TRK antibody cocktail consisting of rabbit monoclonal antibodies, all obtained from Cell Signaling (Danvers, MA), targeting pan-Trk (A7H6R, active against TrkA, TrkB, and TrkC, 1:50 dilution), ROS1 (D4D6, 1:50), and ALK (D5F3, 1:50), as described previously.[29] All the other primary antibodies used are summarized in Table 1. The bound antibodies were visualized using the ultraView Universal DAB Detection Kit (Roche) and the ultraView Universal Alkaline Phosphatase Red Detection Kit (Roche). The slides were counterstained with the Mayer hematoxylin. Appropriate positive and negative controls were used.

TABLE 1. Antibodies Used for Immunohistochemical Study

Antibody Specificity	Clone	Dilution	Antigen Retrieval/ Time (min)	Source
S100 protein	Polyclonal	RTU	CC1/20	Ventana
MMG	304-1A5	RTU	CC1/36	DakoCytomation
CK7	OV-TL 12/30	1:200	CC1/36	DakoCytomation
p63	4A4	RTU	CC1/64	Ventana
DOG1	SP31	RTU	CC1/36	Cell Marque
GATA-3	L50-823	1:200	CC1/52	BioCareMedical
SOX10	Polyclonal	1:100	CC1/64	Cell Marque
Pan-TRK	A7H6R	1:20	CC1/64	Cell Signaling
MIB1	30-9	RTU	CC1/64	Ventana
MYB	EP769Y	1:100	CC1/36	Abcam

CC1—EDTA buffer, pH 8.6.
RTU indicates ready to use.

All cases were analyzed by NGS using the FusionPlex Solid Tumor kit (ArcherDX). All 49 cases of SC were also tested for *ETV6*, *RET*, and *NTRK3* break by fluorescence in situ hybridization (FISH) and for the common *ETV6-NTRK3* fusion using reverse transcription polymerase chain reaction (RT-PCR).

Molecular Genetic Studies

Sample Preparation for NGS and RT-PCR

For NGS and RT-PCR analysis, 2 to 3 formalin-fixed, paraffin-embedded (FFPE) sections (10 μm thick) were macrodissected to isolate tumor-rich regions. Samples were extracted for total nucleic acid using the Agencourt FormaPure Kit (Beckman Coulter, Brea, CA). Both the RNA integrity assessment and detailed description of the analysis carried out using the Archer FusionPlex Solid Tumor Kit were reported previously by our group.[29]

RNA Integrity Assessment and Library Preparation for NGS

Unless otherwise indicated, 250 ng of FFPE RNA was used as an input for NGS library construction. To assess RNA quality, the PreSeq RNA QC Assay using iTaq Universal SYBR Green Supermix (Biorad, Hercules, CA) was performed on all samples during library preparation to generate a measure of the integrity of RNA (in the form of a

cycle threshold [C_t] value). Library preparation and RNA QC were performed following the Archer FusionPlex Protocol for Illumina (ArcherDX Inc.). The Archer FusionPlex Solid Tumor Kit was used. Final libraries were diluted 1:100,000 and quantified in a 10 μL reaction following the Library Quantification for Illumina Libraries protocol and assuming a 200 bp fragment length (KAPA, Wilmington, MA). The concentration of final libraries was around 200 nM. The threshold representing the minimum molar concentration for which sequencing can be robustly performed was set at 50 nM.

NGS Sequencing and Analysis

Libraries were diluted to 4 nM and sequenced on a NextSeq sequencer (Illumina, San Diego, CA). The optimal number of raw reads per sample was set to 3 million. Library pools were diluted to 1.6 pM library stock with 20% 1.8 pM PhiX and loaded in the NextSeq cartridge. The fusion and other rearrangement detection algorithm of Archer Analysis relies on the specificity of the gene-specific primers used in the amplification steps in the AMP process. The resulting FASTQ files were analyzed using the Archer Analysis software (version 5.1.7; ArcherDX Inc.).

Detection of Alterations of ETV6, NTRK3, and RET Genes by the FISH Method

Four-micron-thick FFPE sections were placed onto positively charged slides. Hematoxylin and eosin–stained slides were examined for determination of areas for cell counting. The unstained slides were routinely deparaffinized and incubated in the ×1 Target Retrieval Solution Citrate at pH 6 (Dako, Glostrup, Denmark) and at 95°C for 40 minutes and subsequently cooled for 20 minutes at room temperature in the same solution. Slides were washed in deionized water for 5 minutes and digested in protease solution with pepsin (0.5 mg/mL; Sigma Aldrich, St Louis, MO) in 0.01 M HCl at 37°C for 25 to 60 minutes, according to the sample conditions. Slides were then placed in deionized water for 5 minutes, dehydrated in a series of ethanol solutions (70%, 85%, and 96% for 2 min each), and air dried.

Two commercial probes were used for the detection of rearrangement of *ETV6* and *RET* genes, the Vysis ETV6 Break-Apart FISH Probe Kit (Vysis/Abbott Molecular, IL), and ZytoLight SPEC RET Dual Color Break-Apart Probe (ZytoVision GmbH, Bremerhaven, Germany). The *ETV6* probe was mixed with water and LSI/WCP (Locus-Specific Identifier/Whole Chromosome Painting) Hybridization buffer (Vysis/Abbott Molecular) in a 1:2:7 ratio, respectively. The *RET* probe was factory premixed. Probes for the detection of rearrangement of the *NTRK3* gene region were mixed from custom-designed SureFISH probes (Agilent Technologies Inc., Santa Clara, CA). Chromosomal regions for *NTRK3* break-apart probe oligos are chr15:87501469-88501628 and chr15:88701444-89700343. Probe mixture was prepared from the corresponding probes (each color was delivered in a separate well), deionized water, and LSI Buffer (Vysis/Abbott Molecular) in a 1:1:1:7 ratio, respectively.

An appropriate amount of mixed and premixed probes was applied on the specimens, covered with a glass coverslip, and sealed with rubber cement. Slides were incubated in the ThermoBrite instrument (StatSpin/Iris Sample Processing, Westwood, MA) with codenaturation at 85°C for 8 minutes and hybridization at 37°C for 16 hours. The rubber cemented coverslip was then removed and the slide was placed in a posthybridization wash solution (2×SSC/0.3% NP-40) at 72°C for 2 minutes. The slide was air dried in the dark, counterstained with 4′,6′-diamidino-2-phenylindole (DAPI; Vysis/Abbott Molecular), coverslipped, and examined immediately.

FISH Interpretation

The sections were examined with an Olympus BX51 fluorescence microscope (Olympus Corporation, Tokyo, Japan) using a ×100 objective and filter sets Triple Band Pass (DAPI/SpectrumGreen/SpectrumOrange), Dual Band Pass (SpectrumGreen/SpectrumOrange), and Single Band Pass (SpectrumGreen or SpectrumOrange). For each probe, 100 randomly selected nonoverlapping tumor cell nuclei were examined for the presence of yellow or green and orange fluorescent signals. For the break-apart probe, yellow signals were considered negative, and separate orange and green signals were considered positive. Cutoff values for the break-apart probes were set at >10% of nuclei with chromosomal breakpoint signals (mean+3 SD in normal non-neoplastic control tissues).

RESULTS

Clinical Characteristics

Among the 49 studied cases, 37 (76%) occurred in the parotid gland, 7 (14%) in the submandibular gland, 2 (4%) in the minor salivary glands, and 1 (2%) each in the nasal mucosa, facial skin, and thyroid gland. The majority of cases were diagnosed in males (27; 55%). Patient age at diagnosis varied from 15 to 80 years, with a mean age of 49.9 years. Six SC cases were previously published.[13,29,32,33] The clinicopathologic, immunohistochemical, and molecular genetic findings of all 49 SC cases are summarized in Table 2.

Pathologic Features and Immunophenotype

The typical histologic features seen in most *ETV6-NTRK3* fused SC included solid and microcystic growth pattern with a multilobular architecture divided by thin fibrous septa (Fig. 1A). The tumors either lacked a capsule (42/48; 86%) or were only partially encapsulated (7/48; 14%), mostly showing prominent infiltrative borders (31/48; 65%). The tumor cells had vesicular low-grade nuclei with finely granular chromatin and distinctive centrally located nucleoli, surrounded by pale pink granular or vacuolated cytoplasm. Most SC cases were predominantly composed of solid and microcystic (30/49; 61%) and slightly dilated glandular spaces filled with a variable amount of eosinophilic homogenous secretory material (Fig. 1B). A less common growth pattern previously seen in SCs harboring the *ETV6-RET* gene fusion,[29] comprised a prominent fibrosclerotic stroma with isolated tumor cells in small islands or trabeculae, which were often seen in the central part of the tumor (Fig. 1C). Such a prominent sclerotic stroma was present in 5 of 8 (60%) *ETV6-RET* translocated SCs, but focal hyalinized stromal septa were seen in many other SCs including cases with *ETV6-NTRK3* fusion (Table 2).

TABLE 2. Clinicopathologic, IHC, and Molecular Genetic Findings in 49 Cases of SC Analyzed by NGS[13,29,32,33]

Case No.	Age (y)	Sex	Site	Type of Growth	Fibrous Septa/ Hyalinization	Capsule/ Invasion	IHC S100	IHC MMG	NGS	FISH	RT-PCR
1	56	Female	Parotid	Solid, microcystic	Yes/yes	Invasion	3+	3+	*VIM-RET*	ND	*VIM-RET*
2	60	Male	Submandibular gland	Solid	Yes/yes	Invasion	3+	2+	*ETV6-NTRK3* *MYB-SMR3B*	ND	*ETV6-NTRK3*
3[32]	47	Female	Parotid left	Glandular, macrocystic	NA/NA	Invasion	3+	3+	*ETV6-NTRK3*	*ETV6-NTRK3*	*ETV6-NTRK3*
4[32]	37	Male	Submandibular gland right	Tubular, glandular	Yes/yes	Invasion	3+	3+	*ETV6-NTRK3*	*ETV6-NTRK3*	NA, neg
5	49	Male	Parotid left	Solid, microcystic	Yes/no	Circumscribed	3+	3+	*ETV6-NTRK3*	ND	ND
6	46	Female	Parotid	Solid, microcystic	Yes/yes*	Invasion	3+	3+	*ETV6-RET*	Neg	Neg
7	52	Male	Parotid	Solid, papillary	No/yes	Invasion	2+	3+	*ETV6-NTRK3*	*ETV6*	*ETV6-NTRK3*
8	67	Male	Submandibular gland	Cystic	No/no	Circumscribed	3+	2+	*ETV6-NTRK3*	*ETV6*	Neg
9	51	Female	Nasal mucosa	Tubular, microcystic, papillary	Yes/no	Invasion	1+	1+	*ETV6-NTRK3*	*ETV6*	Neg
10	52	Male	Parotid	Microcystic, lobular solid	Yes/no	Invasion	2+	3+	*ETV6-NTRK3*	*ETV6*	*ETV6-NTRK3*
11	36	Male	Parotid	Lobular solid, papillary, microcystic	Yes/yes	Invasion	2+	ND	*ETV6-NTRK3*	*ETV6*	*ETV6-NTRK3*
12	21	Male	Parotid	Nodular, cystic	Yes/no	Circumscribed	2+	ND	*ETV6-NTRK3*	*ETV6*	*ETV6-NTRK3*
13	74	Female	Parotid	Cystic, papillary, apocrine features	Yes/no	Circumscribed	2+	ND	*ETV6-NTRK3*	*ETV6*	*ETV6-NTRK3*
14	53	Female	Parotid right	Multilobular, papillary	Yes/yes	Circumscribed but invasion	2+	2+	*ETV6-NTRK3*	*ETV6*	*ETV6-NTRK3*
15	35	Female	Parotid right	Cystic, micropapillary, tubular	Yes/yes	Circumscribed	1+	1+	*ETV6-NTRK3*	*ETV6*	*ETV6-NTRK3*
16	15	Male	Parotid left	Multilobular solid	Yes/yes	Invasion	2+	3+	*ETV6-NTRK3*	*ETV6*	*ETV6-NTRK3*
17	26	Female	Submandibular gland left	Multicystic, solid, micropapillary	Yes/yes	Circumscribed but invasion	1+	3+	*ETV6-NTRK3*	*ETV6*	*ETV6-NTRK3*
18	47	Female	Parotid right	Macrocystic, solid, microcystic	No/no	Partially encapsulated	2+	3+	*ETV6-NTRK3*	NA	NA
19	59	Female	Lower lip mucosa	Nodular, solid, microcystic	No/no	Encapsulated	1+	3+	*ETV6-NTRK3*	*ETV6*	*ETV6-NTRK3*
20	52	Male	Parotid right	Lobular, solid, microcystic, macrocystic, papillary	Yes/yes	Circumscribed, partially encapsulated	1+	1+	*ETV6-NTRK3*	*ETV6*	*ETV6-NTRK3*
21	30	Female	Parotid left	Cystic, microcystic, papillary, apocrine	No/no	Circumscribed	1+	3+	*ETV6-NTRK3*	*ETV6*	*ETV6-NTRK3*
22	80	Female	Parotid right	Solid, microcystic	Yes/yes	Circumscribed partially encapsulated	2+	3+	*ETV6-NTRK3*	*ETV6*	*ETV6-NTRK3*
23	77	Female	Parotid right	Solid, microcystic	Yes/yes	Circumscribed	3+	2+	*ETV6-NTRK3*	*ETV6*	*ETV6-NTRK3*
24	60	Male	Parotid right	Multinodular, micropapillary, microcystic	Yes/yes	Circumscribed but invasion	3+	3+	*ETV6-NTRK3*	*ETV6*	*ETV6-NTRK3*
25	66	Male	Thyroid gland left	Solid microcystic, tubular, papillary, apocrine	Yes/yes	Circumscribed but invasion	1+	3+	*ETV6-NTRK3*	*ETV6-NTRK3*	ND
26[33]	34	Male	Parotid	Solid microcystic, papillary	No/yes	Circumscribed	2+	3+	*ETV6-RET*	*ETV6-RET*	ND
27	52	Female	Parotid	Solid microcystic	Yes/yes	Invasion	3+	1+	*ETV6-NTRK3*	*ETV6-NTRK3*	ND
28	60	Female	Parotid right	Solid microcystic, apocrine features	No/yes	Circumscribed but invasion	1+	3+	*ETV6-NTRK3*	*ETV6*	Neg
29	66	Male	Parotid right	Solid microcystic, tubular, papillary	Yes/yes	Invasion	3+	3+	*ETV6-NTRK3*	*ETV6-NTRK3*	Neg
30	20	Female	Submandibular gland	Solid microcystic	Yes/yes	Invasion	2+	3+	*ETV6-NTRK3*	NA	Neg
31	48	Female	Parotid right	Solid microcystic, tubular, papillary	Yes/yes	Invasion	1+	1+	*ETV6-NTRK3*	*ETV6*	ETV6-NTRK3
32	28	Female	Parotid right	Solid microcystic	Yes/yes*	Invasion	1+	3+	*ETV6-RET*	*ETV6-RET*	Neg
33	26	Female	Parotid	Micropapillary, microcystic, apocrine	Yes/no	Invasion	1+	2+	*ETV6-NTRK3*	*ETV6*	Neg
34	55	Male	Parotid	Microcystic micropapillary	Yes/yes*	Circumscribed but invasion	1+	2+	*ETV6-RET*	NA	Neg
35	58	Male	Parotid	Solid microcystic, multilobular	Yes/yes	Invasion	2+	3+	*ETV6-NTRK3*	NA	Neg
36	54	Female	Parotid	Solid microcystic, multilobular	Yes/yes	Invasion	3+	2+	*ETV6-NTRK3*	ND	Neg
37	74	Male	Parotid	Cystic, solid	Yes/yes	Circumscribed	2+	3+	*ETV6-NTRK3*	ND	Neg
38	43	Male	Parotid	Solid microcystic, papillary, apocrine	Yes/yes	Invasion	1+	3+	*ETV6-NTRK3*	ND	Neg

TABLE 2. (*continued*)

Case No.	Age (y)	Sex	Site	Type of Growth	Fibrous Septa/ Hyalinization	Capsule/ Invasion	IHC S100	IHC MMG	NGS	FISH	RT-PCR
39	51	Male	Parotid	Solid microcystic lobular	Yes/yes	Circumscribed but invasion	2+	3+	*ETV6-NTRK3*	ND	Neg
40	73	Male	Parotid	Cystic, solid	No/yes	Circumscribed encapsulated	2+	3+	*ETV6-NTRK3*	*ETV6*	Neg
41	66	Male	Parotid	Solid papillary	Yes/yes	Encapsulated	3+	ND	*ETV6-NTRK3*	*ETV6*	Neg
42[29]	77	Male	Submandibular gland	Cribriform, cystic papillary	Yes/yes	Circumscribed encapsulated	3+	1+	*ETV6-RET*	*ETV6-RET*	Neg
43	39	Female	Palate	Solid microcystic	NA	NA	3+	3+	*ETV6-NTRK3*	NA	Neg
44[29]	31	Male	Submandibular gland	Lobular, microcystic, solid	Yes/yes*	Invasion	3+	3+	*ETV6-RET*	*ETV6*	Neg
45[13]	73	Male	Parotid	Solid, microcystic	Yes/yes	Invasion	3+	3+	*ETV6-NTRK3*	*ETV6*	ETV6-NTRK3
46	41	Male	Parotid	Cystic papillary	No/no	Circumscribed encapsulated	1+	ND	*ETV6-NTRK3*	NA	Neg
47	20	Female	Parotid	Solid microcystic, tubular	Yes/no	Circumscribed but invasion	3+	ND	*ETV6-RET*	*RET*	Neg
48	78	Male	Facial skin	Cystic, cribriform, tubular	Yes/yes	Invasion	2+	Neg	*ETV6-NTRK3*	ND	ND
49	29	Male	Parotid left	Solid, microcystic	Yes/yes*	Circumscribed but invasion	3+	3+	*ETV6-RET*	*ETV6-RET*	Neg

*Prominent fibrosclerotic stroma.
Scoring system for assessment of IHC stainings for S100 protein and MMG: 1+, <50%; 2+, 50% to 75%; 3+, 75% to 100%.
IHC indicates immunohistochemistry; NA, not available; ND, not done; neg, negative.

SC with high-grade (HG) transformation consisted of 2 distinct sharply delineated carcinomatous components (Fig. 1D). One was a conventional SC composed of uniform neoplastic cells arranged in solid, tubular, and microcystic growth structures, divided by fibrous septa that were partly hyalinized. In contrast, the HG component appeared as a distinct population of anaplastic cells arranged in trabecular patterns, and with common perineurial invasion (Fig. 1D). Irregular-shaped tumor islands with large geographic comedo-like necrosis were often seen in the HG component of SC. The tumor cells herein showed nuclear pleomorphism, distinctive nucleoli and they lacked secretory activity (Fig. 1E).

Yet another growth pattern, seen in both *ETV6-NTRK3* and *ETV6-RET* fused SC cases, was a predominantly multicystic one (6/49; 12%). The cysts were lined mostly by a single or focally a double layer of cells with prominent apocrine differentiation; hobnail cells and vacuolated foamy cells were present as well (Fig. 1F). Very rare SCs were well circumscribed and surrounded by a thick, fibrous capsule, composed of 1 single cystic space that contained abundant proteinaceous eosinophilic material (3/49; 6%). Histologic findings are summarized in Table 2.

Immunohistochemical Findings

By immunohistochemistry, most examined cases were strongly and diffusely positive for S100 protein (Fig. 2A) and MMG (Fig. 2B). Both markers also stained the secretory material. In particular, immunostaining for S100 protein was seen in all cases of SC. Strong and diffuse nuclear-cytoplasmic expression in almost all neoplastic cells was seen in 19 (39%) cases, and intermediate positivity in 16 (33%) cases and mild in 14 (28%) cases. MMG was strongly expressed in 29 SCs (59%); intermediate and mild positivity was encountered in 7 (14%) and 6 (12%) cases, respectively. Immunohistochemical findings of S100 and MMG are presented in Table 2. Other expressed antibodies included CK7 (Fig. 2C), GATA-3, and SOX10 (Fig. 2D). The p63 protein was negative in most cases, but showed limited areas of positive peripheral myoepithelial cell staining suggestive of a focal intraductal component in 3 cases. DOG1 was negative in all examined cases. Proliferative activity was generally low, with a mean MIB-1 index of 15% (range: 5% to 40%).

Index Case 1: Salivary SC With a Novel VIM-RET Fusion

Histologically, this case featured a typical SC morphology, characterized by a predominantly solid and microcystic growth pattern with a multilobular architecture divided by thin fibrous septa (Fig. 3A). Perineurial growth was noted (Fig. 3B). Some areas showed macrocystic transformation. The cystic spaces were lined by a single layer of neoplastic cells and contained an eosinophilic material (Fig. 3C). Dense hyalinization with isolated tumor cell nests was present in some areas (Fig. 3D). Tumor cells were diffusely positive for MMG (Fig. 3E) and S100 protein (Fig. 3F).

Index Case 2: Salivary SC With Dual ETV6-NTRK3 and Novel MYB-SMR3B Fusions

SC of the submandibular gland showed a multifocal and widely invasive growth pattern in the submandibular gland (Fig. 4A). The tumor had a predominantly solid architecture; hyalinization and sclerotic areas were prominent. In some areas, the desmoplastic stroma surrounded isolated tumor cell nests. The neoplastic cells showed a nuclear pleomorphism and minimal residual secretory activity (Fig. 4B). Occasional comedo-like necrosis was present (Fig. 4C). A cytology specimen featured a pleomorphic cell population, with prominent nuclei and nuclear grooves (Fig. 4D). The cells had a high mitotic activity with an MIB-1 index of 40% (Fig. 4E). By immunohistochemistry, S100 protein, CK7, MMG, SOX10,

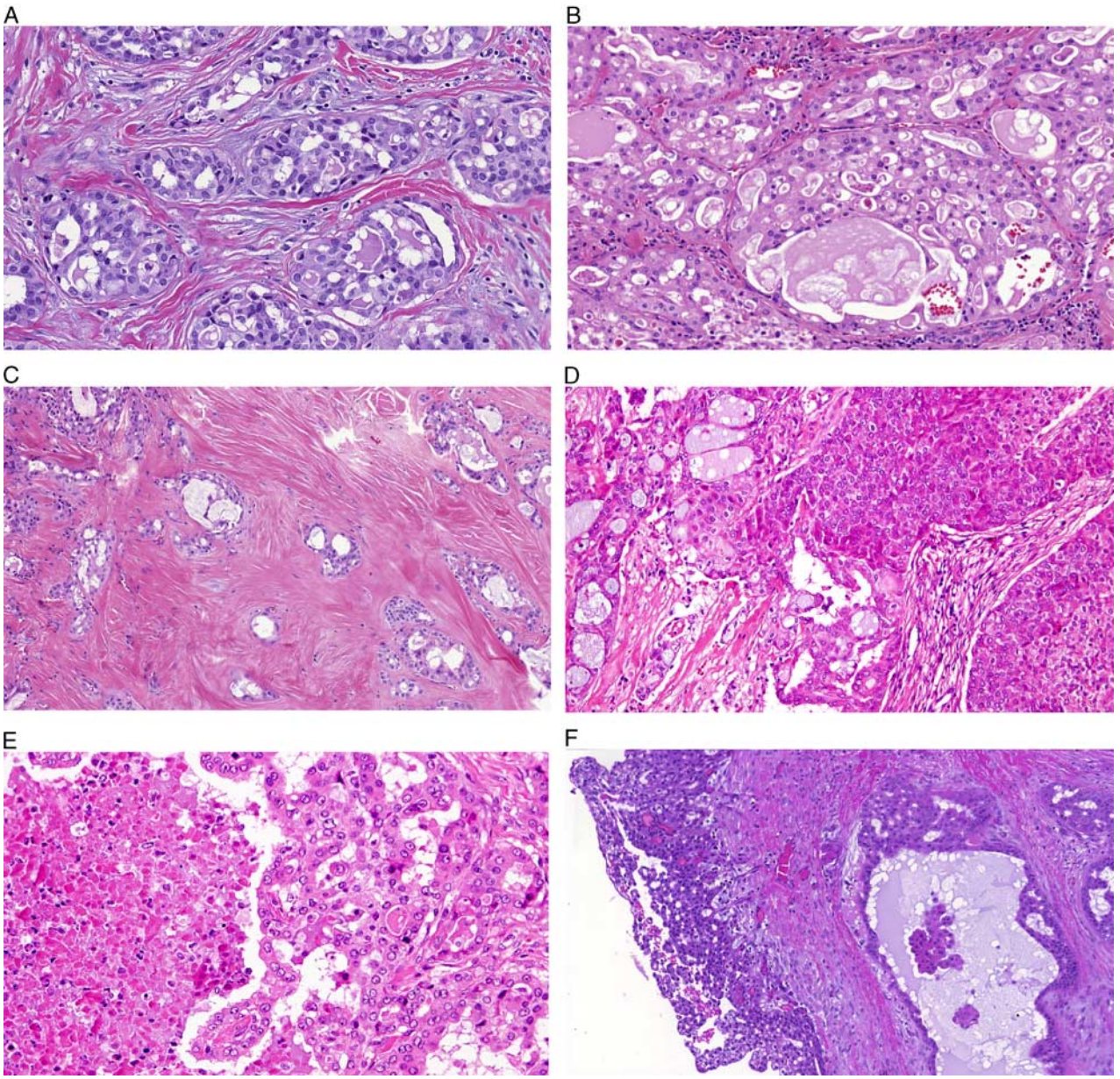

FIGURE 1. Major growth patterns in SC cases. A, Most *ETV6-NTRK3* fused SC showed a solid and microcystic growth pattern with a multilobular architecture divided by thin fibrous septa. B, SC composed of dilated glandular spaces filled with a variable amount of eosinophilic homogeneous secretory material. C, Usually centrally located prominent fibrosclerotic stroma permeated by isolated small islands or trabeculae of tumor cells. Overall, this pattern is rarely encountered in MASC, but is overrepresented in cases with *ETV6-RET* fusion. D, SC with HG transformation consisted of 2 distinct sharply delineated carcinomatous components. E, Irregular-shaped tumor islands with large geographic comedo-like necrosis are seen in the HG component of SC. Tumor cells in HG areas display apparent nuclear pleomorphism, prominent nucleoli and they lack any secretory activity. F, Predominantly multicystic growth pattern seen in both *ETV6-NTRK3* and *ETV6-RET* SC cases. The cysts were lined mostly by a single or focally a double layer of cells with prominent apocrine differentiation; hobnail and vacuolated foamy cells were present as well.

CK7, and pan-TRK were diffusely positive in all neoplastic cells. Nuclear staining for MYB was found in most neoplastic cells (Fig. 4F).

Index Case 3: SC of Thyroid Gland

This tumor was predominantly microcystic, with some areas showing fusion of the microcysts, thereby creating a cribriform pattern. Eosinophilic to basophilic secretions with scalloped edges were diffusely present within the microcysts. Focally dilated cysts containing variably thick and sometimes edematous fibrovascular cores were present. From these fibrovascular cores emanated nonhierarchically branched micropapillae, focally forming a "medusa head"-type appearance. The stroma was sclerotic to desmoplastic. The pushing type of

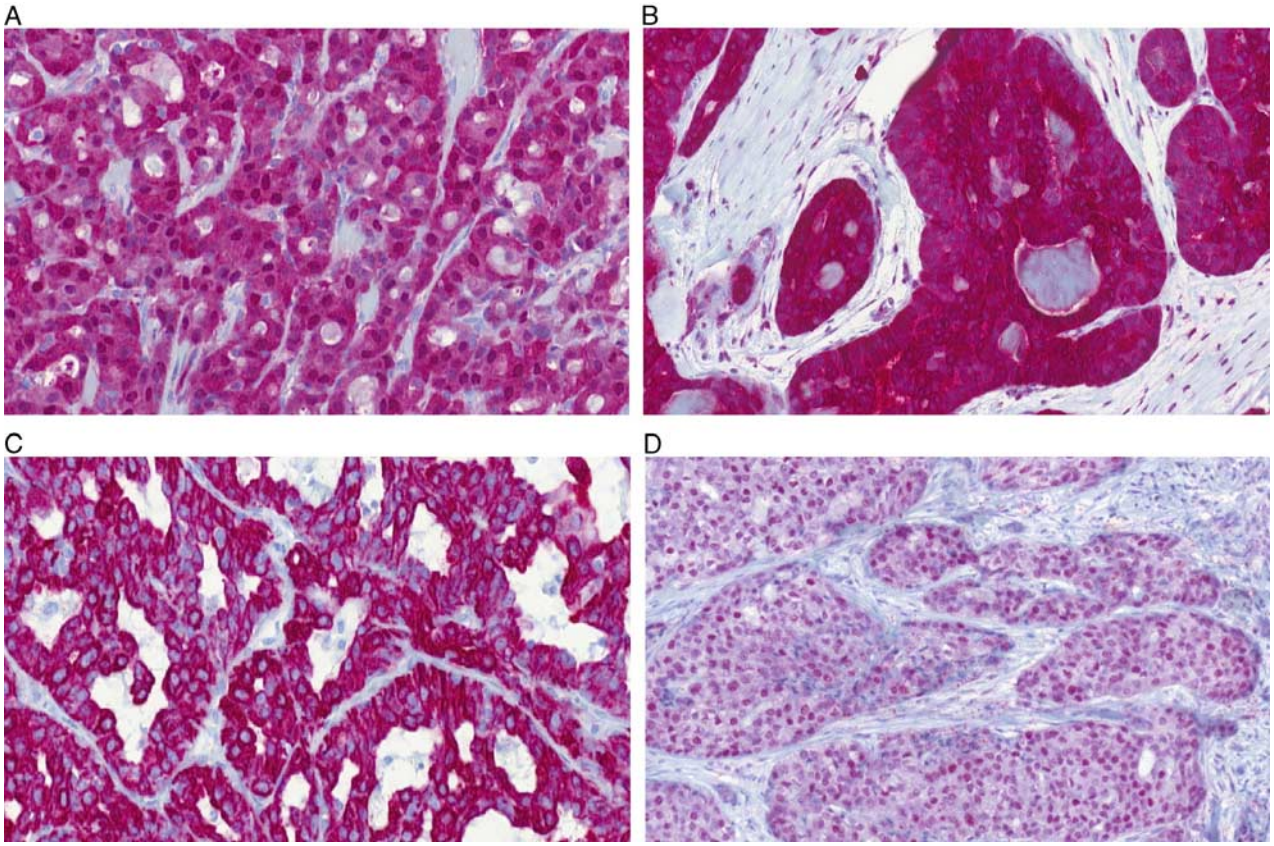

FIGURE 2. Immunohistochemical findings in the SC cohort. A–D, All studied cases showed typical immunohistochemical features of SC. The tumor cells showed membranous and nuclear S100 (A) and MMG (B) positivity, membranous CK7 (C) positivity, and nuclear SOX10 (D) positivity.

invasion predominated and extended into extrathyroidal tissue including skeletal muscle. Focally, small neoplastic tubular formations irregularly invaded into the surrounding tissues as well. Nuclei of the neoplastic cells were uniform, low grade, and oval, with a single inconspicuous to medium-sized nucleolus. Although nuclear grooves were present, no nuclear pseudoinclusions were seen and the chromatin patterns and nuclear size were distinct from conventional papillary thyroid carcinoma. Cytoplasm was amphophilic to eosinophilic. Focal apocrine snouts were noted. No necrosis or HG transformation was identified. MMG and S100 protein, and GATA-3, were diffusely expressed. TTF-1, thyroglobulin, PAX8, and NKX3.1 were all negative. A break-apart FISH study for *ETV6* was positive; NGS analysis revealed *ETV6-NTRK3* fusion confirmed by RT-PCR.

Molecular Findings and Clinicopathologic Correlates

Forty SC cases (82%) presented the classic *ETV6-NTRK3* fusion. Of the 9 *ETV6-NTRK3* fusion-negative cases, 8 presented with an *ETV6-RET* fusion. A novel *VIM-RET* fusion transcript was identified in 1 case of SC of the parotid gland (Fig. 5A) by NGS analysis. In addition, 1 recurrent HG SC of the submandibular gland was positive for both *ETV6-NTRK3* and *MYB-SMR3B* fusion transcripts (Fig. 5B). In the FISH analysis, *ETV6* splits were detected in 33/49 (67%), *NTRK3* splits in 5/49 (10%), and RET rearrangement in 5/49 (10%) (Table 2). The *ETV6-NTRK3* fusion was confirmed in 19 SCs (39%) by RT-PCR. The single SC harboring *VIM-RET* fusion was confirmed by RT-PCR as well. All results of molecular testing are summarized in detail in Table 2.

Clinical Outcome Highlighting the Potential for Local Recurrence and Distant Metastasis

Forty-three patients (88%) had clinical follow-up data available, with a median follow-up of 61.2 months (range: 7 to 192 mo). Nine patients developed local recurrence, with multiple recurrences in 2 of the patients between 12 and 36 months after initial surgery. Six patients in our cohort died, 3 of them at 24, 42, and 50 months after primary surgery due to metastatic disease with multiple distant metastases to lymph nodes, bones, and lungs, whereas the remaining 3 patients died of other unrelated causes with no evidence of tumor. Three patients are alive with recurrent or residual disease at 48, 60, and 187 months of follow-up. The remaining 34 patients were disease and recurrence free at the lastest contact, with a median follow-up of 45 months after primary diagnosis (range: 7 to 192 mo). Follow-up was unavailable in 6 cases. No patient has received treatment with TRK inhibitors so far.

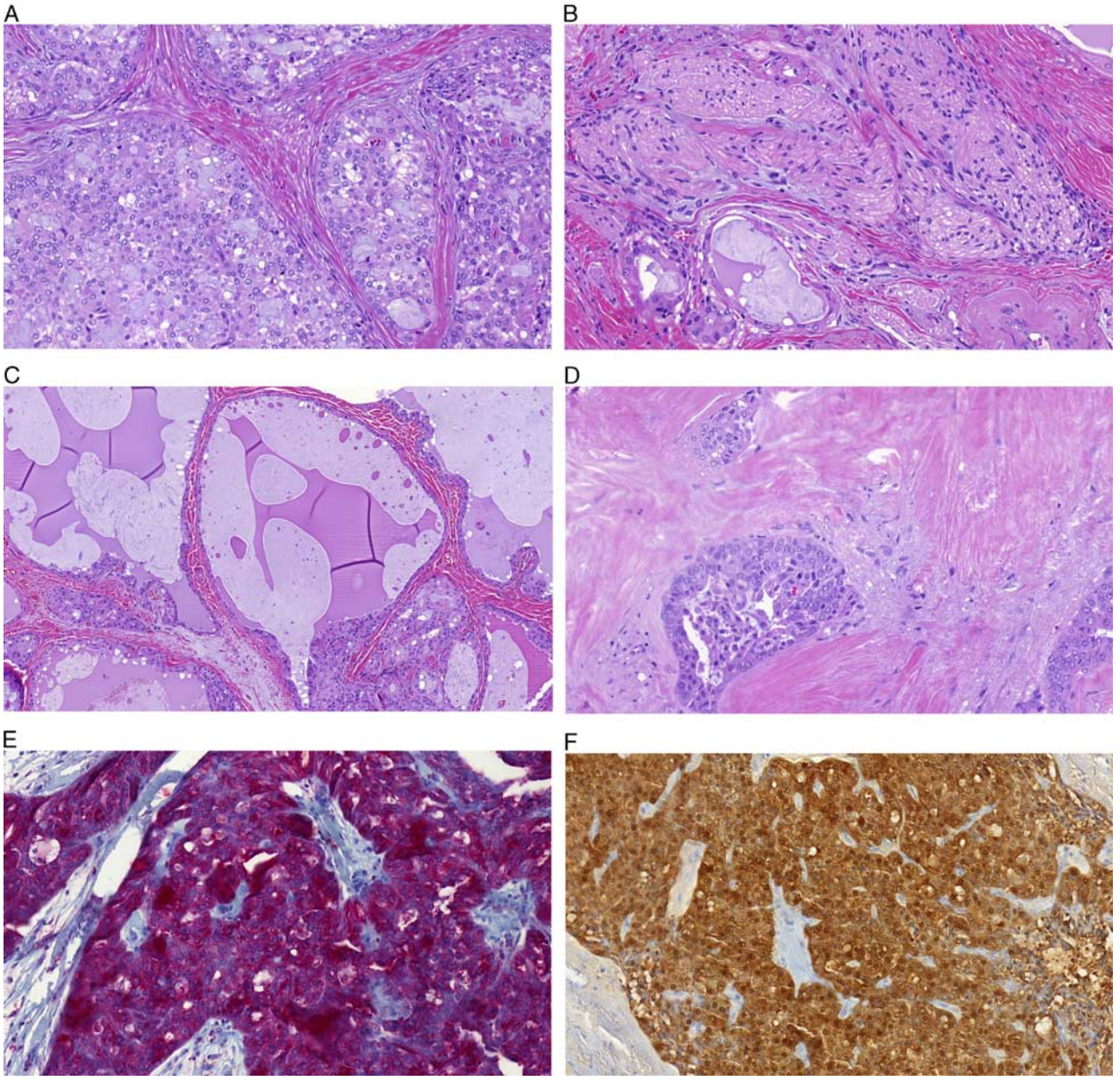

FIGURE 3. SC with *VIM-RET* fusion. A, SC of the parotid gland characterized by solid and microcystic growth. Thin fibrous septa separate the tumor into multiple nodules. B, Perineurial growth was noted. C, Some areas showed macrocystic transformation. The cystic spaces were lined by a single layer of neoplastic cells and contained an eosinophilic material. D, Dense hyalinization with isolated tumor cell nests was present in some areas. Tumor cells were diffusely positive for MMG (E) and S100 protein (F).

Index Case 1: Salivary SC With a Novel VIM-RET Fusion

A 56-year-old woman presented with a slowly growing mass in the parotid gland. Superficial parotidectomy was performed and the tumor was removed completely with free surgical margins. The patient refused any additional treatment. Twenty months after surgery, the patient is well, without clinical or radiologic signs of tumor recurrence.

Index Case 2: Salivary SC With Dual ETV6-NTRK3 and Novel MYB-SMR3B Fusions

A 61-year-old man presented with a recurrent tumor of the right submandibular gland measuring 1.9×1.5×1.0 cm. The affected salivary gland was resected and the patient underwent 35 rounds of radiotherapy. Four years later, the patient developed a tumor recurrence in the adjacent tissues in the right side of the neck. Lymph node dissection was performed and a single metastatic lymph

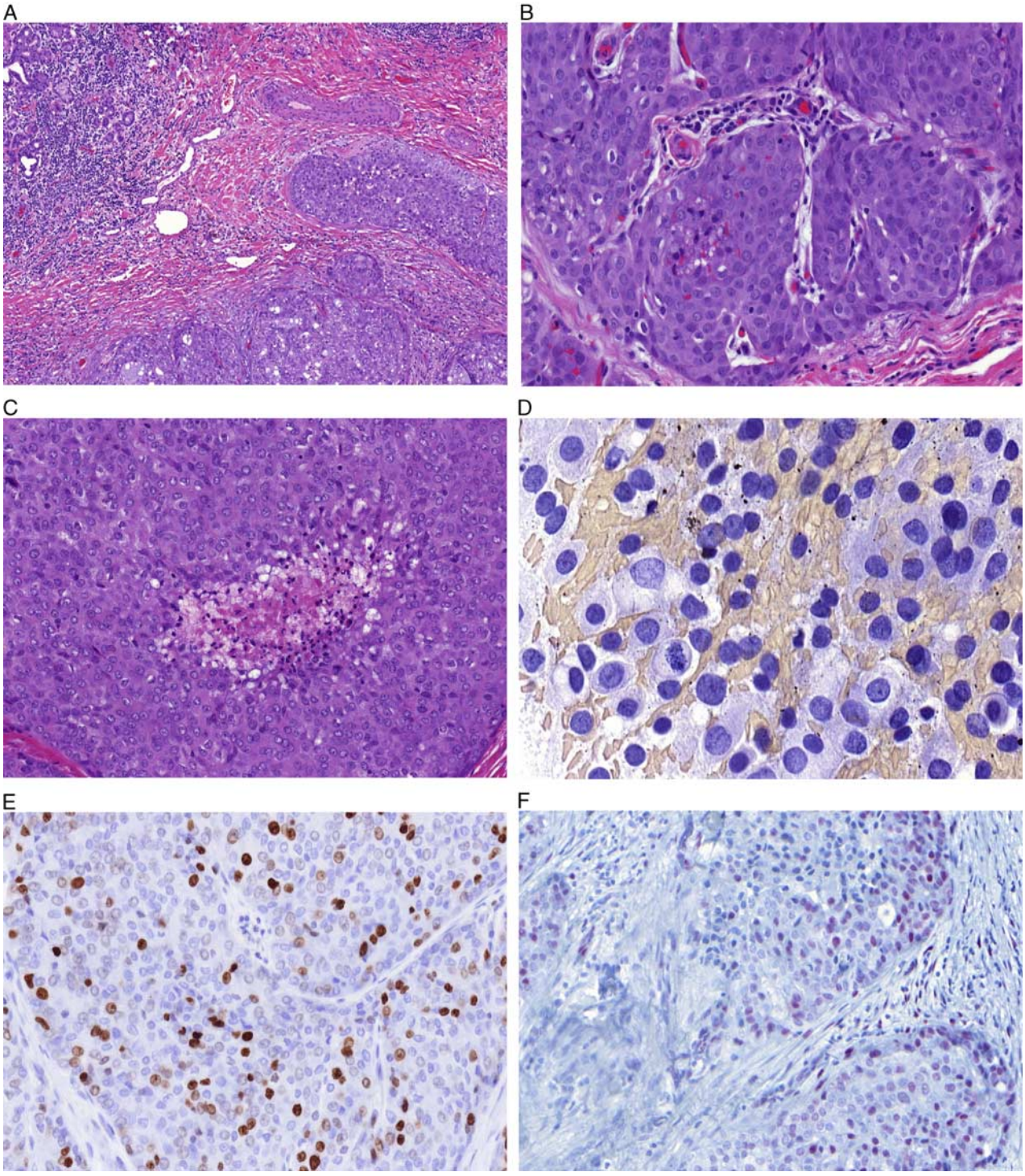

FIGURE 4. SC with dual *ETV6-NTRK3* and *MYB-SMR3B*. A, SC of the submandibular gland showed multifocal and widely invasive growth into the residual normal glandular structures. B, Hyalinization and sclerotic areas were prominent and separated the areas of low-grade tumor cells with minimal residual secretory activity from HG areas composed of isolated tumor nests surrounded by a desmoplastic stroma. C, Comedo-like necrosis was present. D, Cytology preparation (PAP stain) featured a pleomorphic cell population with nuclear grooves, prominent nucleoli, and occasionally mitoses. E, MIB 1 index (Ki-67) was 40%. F, Tumor cells were positive with the MYB antibody.

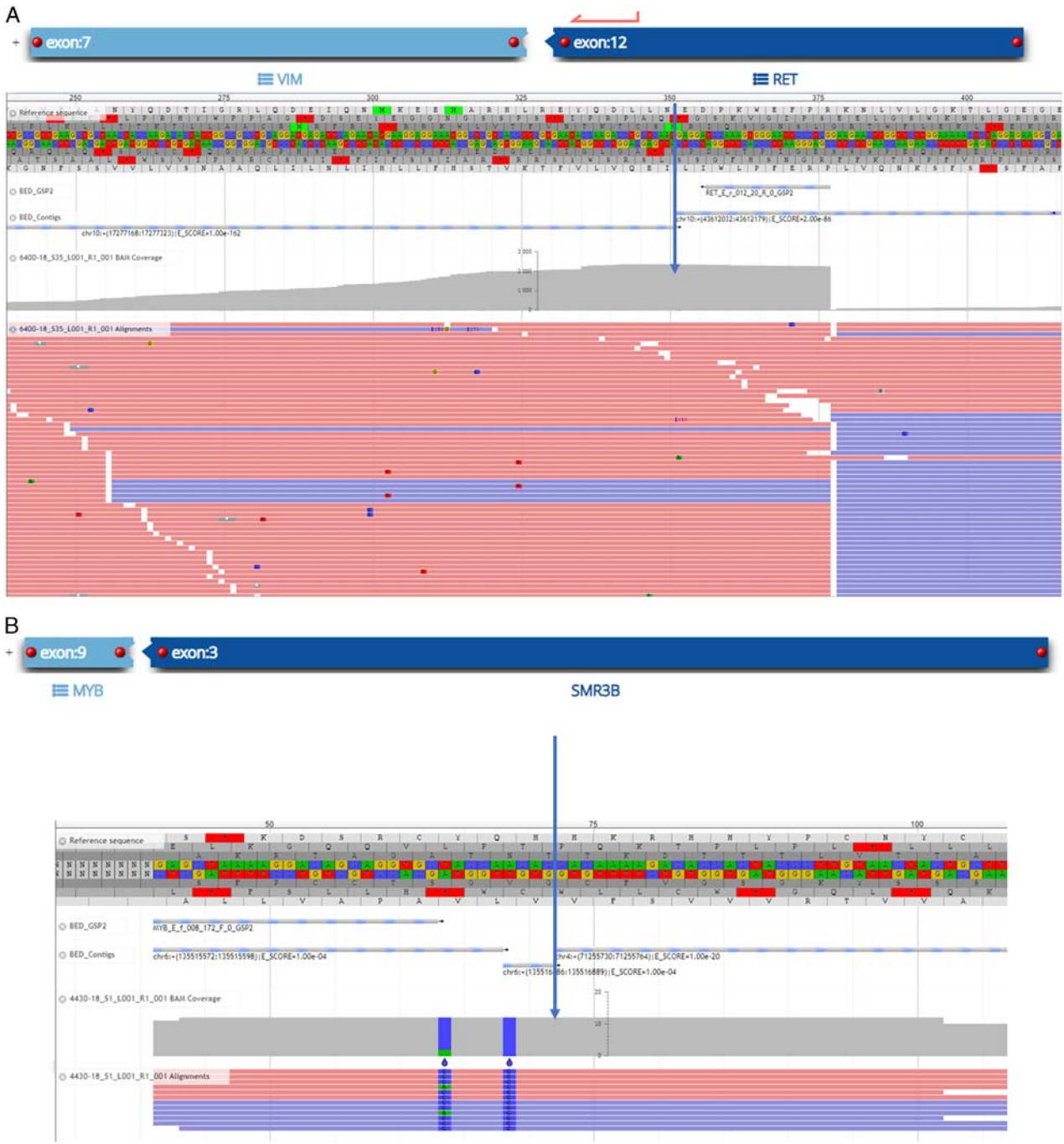

FIGURE 5. Schematic visualization of detected fusion transcripts identified by the ArcherDX assay. A, Fusion involving the VIM exon 7 with RET exon 12 is illustrated along with detailed information about exons joining, coverage of studied region, and about the individual reads. The blue arrow shows the exact breakpoint. B, The fusion involving the *MYB* exon 9 with *SMR3B* exon 3 is illustrated along with detailed information about exons joining, coverage of studied region, and about the individual reads. The blue arrow shows the exact breakpoint.

node was found in 41 investigated lymph nodes of the neck. Postoperative positron emission tomography/computed tomography and lung computed tomography scans were negative. Fourteen months later, a new scar nodule was noted, which was confirmed to be recurrent carcinoma.

Index Case 3: SC of Thyroid Gland With ETV6-NTRK3 Fusion

Sections of a 3.0-cm right thyroid lobe mass in a 66-year-old man with a history of prostate adenocarcinoma showed a multilobulated tumor growing in microcystic and

papillary cystic patterns within the thyroid. Although no lymphovascular space or perineural invasion was identified, metastatic SC histologically identical to the primary thyroid tumor was identified in 2 ipsilateral level 3 nodes. The metastatic deposits measured about 1.5 cm each, with one of them showing a focal limited extranodal extension about 1.0 mm from the node capsule. There were 25 and 5 separate negative lateral neck and level 6 lymph nodes, respectively. The patient underwent adjuvant radiotherapy, which was completed 3 months after thyroidectomy, and is currently alive, with no evidence of recurrence at 36 months of follow-up.

DISCUSSION

A specific chromosomal translocation t(12;15)(p13; q25) resulting in *ETV6-NTRK3* gene rearrangement was initially considered a distinct molecular signature of SC. However, more recent studies have raised the possibility of alternative *ETV6* partners, first published as SCs with *ETV6-X* gene fusions.[27,28] Subsequently, one such alternative rearrangement in a subset of SC was shown to be an *ETV6-RET* gene fusion.[29] The identification of this novel transcript further expanded the molecular diversity of SC and opened the possibility of integrating targeted *RET* inhibitors as a potential therapeutic strategy.

Although most SCs are slow-growing, low-grade malignancies that can be effectively managed by surgery alone, a small subset of SCs may transform into an aggressively growing HG carcinoma.[34] Moreover, even some SCs with low-grade morphology can present with more aggressive behavior that cannot be managed by surgery alone.[29] SCs with the classic *ETV6-NTRK3* gene fusion are well known to respond to new specific *TRK* tyrosine kinase inhibitors Vitrakvi (larotrectinib) and Rozlytrek (entrectinib) or to the second-generation tyrosine kinase inhibitors selitrectinib (LOXO-195)[35] and repotrectinib.[36] A small subset of SCs reveals, however, alternative fusion partners different from *ETV6-NTRK3*, such as *ETV6-RET*[29] and *VIM-RET* gene fusion.[37] These *RET*–fusion-positive tumors would obviously be unreactive to all first-generation and second-generation *TRK*-specific inhibitors. There are, however, specific *RET* inhibitors, such as selpercatinib (LOXO-292) and pralsetinib (Blu-667), under development, which are effective in the treatment of *RET*–fusion-positive tumors, and which are expected to be effective with these *RET*–fusion-positive SCs as well.[38]

The initial description of SC included only *ETV6-NTRK3* gene fusions, but since then, other alternative chimeric fusions have been reported such as *ETV6-RET*, *ETV6-MET*, dual *ETV6-NTRK3*, and *ETV6-MAML3*.[29–31] There is no consensus on whether molecular documentation is an absolute requirement to render the diagnosis of SC, especially in the setting of typical cytopathologic and/or light microscopic features in conjunction with diffuse MMG and S100 protein immunoreactivity.[39] Although the current WHO Classification includes *ETV6-NTRK3* fusion in the definition of SC, it does not, however, state that molecular testing is a requirement for a histopathologic diagnosis of salivary gland tumors.[7] Moreover, there are other salivary gland carcinomas characterized by recurrent translocations and gene rearrangements such as intraductal carcinoma (*NCOA4-RET* and *TRIM27-RET*),[40,41] the cribriform variant of polymorphous (low-grade) adenocarcinoma (*PRKD1-3* rearrangements),[42] clear cell carcinoma (*EWSR1-ATF1*),[43] mucoepidermoid carcinoma (*CRTC1-MAML2*),[44,45] and adenoid cystic carcinoma (*MYB-NFIB*),[46] which do not harbor their respective genetic abnormality in 100% of reported cases. However, the molecular confirmation of both fusion partners is a recommended requirement for aggressive cases where targeted therapies are considered.

Until recently, SC cases with an intact *ETV6* gene were viewed with skepticism. As the molecular profile of SC continues to expand, it would be expected that the *ETV6*-negative cases could result from an alternative genetic abnormality. Several *ETV6*-negative cases were reported in a cohort of macrocystic SCs[16] and also in a subset of SC cases with a more aggressive behavior.[47] Moreover, a novel *NFIX-PKN1* gene fusion was reported recently in 1 case of cutaneous SC.[48] From a routine pathology perspective, our present report of the first non-*ETV6* 5′ fusion partner in salivary SC also carries important implications for the choice of a molecular diagnostic technique. Although traditionally, many challenging diagnostic cases were confirmed molecularly using the *ETV6* FISH break-apart probe, our current finding of the *VIM-RET* fusion renders such a negative FISH result inconclusive. Therefore, along with the increasing clinical interest in the recognition of the particular 3′ fusion gene, it further supports the use of NGS sequencing for SCs where molecular confirmation is necessary for therapeutic choices.

The *VIM* gene, located at chromosome 10p13, encodes for vimentin, a ubiquitous intermediate filament protein of mesenchymal cells, which is, however, also present in some epithelia. Along with microtubules and actin microfilaments, intermediate filaments form part of the cytoskeleton of cells. Overexpression of vimentin has been suggested to signal the onset of epithelial-mesenchymal transformation during cancer progression.[49] The *RET* gene encodes for the well-known receptor tyrosine kinase protein. Although translocations involving the *RET* gene are relatively common in many malignancies,[50] its partnership with the *VIM* gene in gene fusions is infrequent. *VIM* fusions were described, however, in hemangioma[51] and prostate cancer.[52] Importantly, in our SC case, the *VIM* gene joins *RET* in a manner that preserves the tyrosine kinase domain, suggesting oncogenic potential for this fusion.

The second novel gene fusion, which is accompanied by the classic *ETV6-NTRK3* fusion, is *MYB-SMR3B*. The *MYB* gene is a transcription factor and, similar to the previously mentioned *RET*, has been implicated in tumorigenesis of many malignancies.[50] In terms of salivary gland tumors, it forms the well-known *MYB-NFIB* fusion in adenoid cystic carcinoma.[53] In contrast, translocations involving the *SMR3B* gene are rare, and, interestingly, the expression of this gene is nearly exclusive for salivary glands. We can speculate that its fusion with *MYB* may play a role in cancer progression and, perhaps, in acquisition of the HG features in this particular tumor case.

In conclusion, the main novel finding in our study is the discovery of a *VIM-RET* fusion in 1 patient with SC of

the parotid gland. Presumably, this patient might benefit from *RET*-targeted therapy. Furthermore, our finding indicates that a negative *ETV6* FISH result does not rule out SC as a diagnostic alternative. In addition, 1 recurrent HG SC was shown to harbor 2 different fusions: *ETV6-NTRK3* and *MYB-SMR3B*. These novel findings extend the molecular spectrum of SC, and provide a novel insight into its oncogenesis. *VIM-RET* fusion also carries important implications for molecular diagnostics as it represents the first SC-associated gene fusion with a non-*ETV6* 5′ fusion partner.

REFERENCES

1. Skalova A, Vanecek T, Sima R, et al. Mammary analogue secretory carcinoma of salivary glands, containing the *ETV6-NTRK3* fusion gene: a hitherto undescribed salivary gland tumor entity. *Am J Surg Pathol*. 2010;34:599–608.
2. Tognon C, Knezevich SR, Huntsman D, et al. Expression of the *ETV6-NTRK3* gene fusion as a primary event in human secretory breast carcinoma. *Cancer Cell*. 2002;2:367–376.
3. Knezevich SR, McFadden DE, Tao W, et al. A novel *ETV6-NTRK3* gene fusion in congenital fibrosarcoma. *Nat Genet*. 1998;18:184–187.
4. Knezevich SR, Garnett MJ, Pysher TJ, et al. ETV6-NTRK3 gene fusions and trisomy 11 establish a histogenetic link between mesoblastic nephroma and congenital fibrosarcoma. *Cancer Res*. 1998;15:5046–5048.
5. Leeman-Neill RJ, Kelly LM, Liu P, et al. *ETV6-NTRK3* is a common chromosomal rearrangement in radiation-associated thyroid cancer. *Cancer*. 2014;120:799–807.
6. Kralik JM, Kranewitter W, Boesmueller H, et al. Characterization of a newly identified *ETV6-NTRK3* fusion transcript in acute myeloid leukemia. *Diagn Pathol*. 2011;6:19.
7. Skalova A, Bell D, Bishop JA, et al. Secretory carcinoma. In: El-Naggar A, Chan JKC, Grandis JR, Takata T, Slootweg PJ, eds. *World Health Organization (WHO) Classification of Head and Neck Tumours*, 4th edition. IARC Press, Lyon, France. 2017:177–178.
8. Skalova A. Mammary analogue secretory carcinoma of salivary gland origin: an update and expanded morphologic and immunohistochemical spectrum of recently described entity. *Head Neck Pathol*. 2013;7:S30–S36.
9. Skalova A, Gnepp DR, Lewis JS Jr, et al. Newly described entities in salivary gland pathology. *Am J Surg Pathol*. 2017;41:e33–e47.
10. Griffith C, Seethala R, Chiosea SI. Mammary analogue secretory carcinoma: a new twist to the diagnostic dilemma of zymogen granule poor acinic cell carcinoma. *Virchows Arch*. 2011;459:117–118.
11. Fehr A, Loning T, Stenman G. Mammary analogue secretory carcinoma of the salivary glands with *ETV6-NTRK3* gene fusion. Letter to the editor. *Am J Surg Pathol*. 2011;35:1600–1602.
12. Connor A, Perez-Ordoñez B, Shago M, et al. Mammary analog secretory carcinoma of salivary gland origin with the *ETV6* gene rearrangement by FISH: expanded morphologic and immunohistochemical spectrum of a recently described entity. *Am J Surg Pathol*. 2012;36:27–34.
13. Majewska H, Skalova A, Stodulski D, et al. Mammary analogue secretory carcinoma of salivary glands: a new entity associated with *ETV6* gene rearrangement. *Virchows Arch*. 2015;466:245–254.
14. Bishop JA. Unmasking MASC: bringing to light the unique morphologic, immunohistochemical and genetic features of the newly recognized mammary analogue secretory carcinoma of salivary glands. *Head Neck Pathol*. 2013;7:35–39.
15. Bishop JA, Yonescu R, Batista D, et al. Most nonparotid "acinic cell carcinomas" represent mammary analog secretory carcinomas. *Am J Surg Pathol*. 2013;37:1053–1057.
16. Hernandez-Prera JC, Holmes BJ, Valentino A, et al. Macrocystic (mammary analogue) secretory carcinoma an unusual variant and a pitfall in the differential diagnosis of cystic lesions in the head and neck. *Am J Surg Pathol*. 2019;43:1483–1492.
17. Bishop JA, Taube JM, Su A, et al. Secretory carcinoma of the skin harboring *ETV6* gene fusions. A cutaneous analogue to secretory carcinomas of the breast and salivary glands. *Am J Surg Pathol*. 2017;41:62–66.
18. Kazakov DV, Hantschke M, Vanecek T, et al. Mammary-type secretory carcinoma of the skin. *Am J Surg Pathol*. 2010;34:1226–1227.
19. Hyrcza MD, Ng T, Crawford RI. Detection of the *ETV6-NTRK3* translocation in cutaneous mamary-analogue secretory carcinoma. *Diagn Histopathol*. 2015;21:481–484.
20. Lurquin E, Jorissen M, Debiec-Rychter M, et al. Mammary analogue secretory carcinoma of the sinus ethmoidalis. *Histopathology*. 2015;67:749–751.
21. Baneckova M, Agaimy A, Andreassen S, et al. Mammary analog secretory carcinoma of the nasal cavity: characterization of 2 cases and their distinction from other low-grade sinonasal adenocarcinomas. *Am J Surg Pathol*. 2018;42:735–743.
22. Xu B, Aryeequaye R, Wang L, et al. Sinonasal secretory carcinoma of salivary gland with high grade transformation: a case report of this under-recognized diagnostic entity with prognostic and therapeutic implications. *Head Neck Pathol*. 2018;12:274–278.
23. Reynolds S, Shaheen M, Olson G, et al. A case of primary mammary analog secretory carcinoma (MASC) of the thyroid masquerading as papillary thyroid carcinoma: potentially more than a one off. *Head Neck Pathol*. 2016;10:405–413.
24. Dettloff J, Seethala RR, Stevens TM, et al. Mammary analog secretory carcinoma (MASC) involving the thyroid gland: a report of the first 3 cases. *Head Neck Pathol*. 2017;11:124–130.
25. Dogan S, Wang L, Ptashkin RN, et al. Mammary analog secretory carcinoma of the thyroid gland: a primary thyroid adenocarcinoma harboring *ETV6-NTRK3* fusion. *Mod Pathol*. 2016;29:985–995.
26. Huang T, McHugh JB, Berry GJ, et al. Primary mammary analogue secretory carcinoma of the lung: a case report. *Hum Pathol*. 2018;74:109–113.
27. Ito Y, Ishibashi K, Masaki A, et al. Mammary analogue secretory carcinoma of salivary glands: a clinicopathological and molecular study including 2 cases harboring *ETV6-X* fusion. *Am J Surg Pathol*. 2015;39:602–610.
28. Skalova A, Vanecek T, Simpson RHW, et al. Mammary analogue secretory carcinoma of salivary glands. Molecular analysis of 25 *ETV6* gene rearranged tumors with lack of detection of classical *ETV6-NTRK3* fusion transcript by standard RT-PCR: report of 4 cases harboring *ETV6-X* gene fusion. *Am J Surg Pathol*. 2016;40:3–13.
29. Skalova A, Vanecek T, Martinek P, et al. Molecular profiling of mammary analogue secretory carcinoma revealed a subset of tumors harboring a novel *ETV6-RET* translocation: report of 10 cases. *Am J Surg Pathol*. 2018;42:234–246.
30. Rooper LM, Karantanos T, Ning Y, et al. Salivary secretory carcinoma with a novel *ETV6-MET* fusion: expanding the molecular spectrum of a recently described entity. *Am J Surg Pathol*. 2018;42:1121–1126.
31. Guilmette J, Dias-Santagata D, Nose V, et al. Novel gene fusions in secretory carcinoma of the salivary glands: enlarging the *ETV6* family. *Hum Pathol*. 2019;83:50–58.
32. Miesbauerová M, Tommola S, Šteiner P, et al. Cytopathological features of secretory carcinoma of salivary glands and ancillary techniques in its diagnostics: impact of new Milan system for reporting salivary gland cytopathology. *APMIS*. 2019;127:491–502.
33. Stevens TM, Kovalovsky AO, Velosa C, et al. Mammary analog secretory carcinoma, low-grade salivary duct carcinoma, and mimickers: a comparative study. *Mod Pathol*. 2015;28:1084–1100.
34. Skalova A, Vanecek T, Majewska H, et al. Mammary analogue secretory carcinoma of salivary glands with high grade transformation: report of three cases with the *ETV6-NTRK3* gene fusion and analysis of TP53, beta-catenin, EGFR and CCND1 genes. *Am J Surg Pathol*. 2017;38:23–33.
35. Kummar S, Lassen UN. TRK inhibition: a new tumor agnostic treatment strategy. *Targeted Oncology*. 2018;13:545–556.
36. Drilon A. TRK inhibitors in TRK fusion-positive cancers. *Ann Oncol*. 2019;30(suppl 8):viii23–viii30.
37. Skalova A, Santana Conceição T, Vanecek T, et al. Salivary secretory carcinoma with a novel *VIM-RET* fusion: NGS based molecular profiling of 49 cases revealed an expanding molecular spectrum of a recently described entity United States & Canadian Academy of Pathology Annual Meeting 2019/03/01. *Mod Pathol*. 2019;32:1–59.
38. Li AY, McCusker MG, Russo A, et al. *RET* fusions in solid tumors. *Cancer Treat Rev*. 2019;81:101911.

39. Shah AA, Wenig BM, LeGallo RD, et al. Morphology in conjunction with immunohistochemistry is sufficient for the diagnosis of mammary analogue secretory carcinoma. *Head Neck Pathol*. 2015;9:85–95.
40. Skálová A, Ptáková N, Santana T, et al. *NCOA4-RET* and *TRIM27-RET* are characteristic gene fusions in salivary intraductal carcinoma, including invasive and metastatic tumors. Is intraductal correct? *Am J Surg Pathol*. 2019;43:1303–1313.
41. Skalova A, Vanecek T, Uro-Coste E, et al. Molecular profiling of salivary gland intraductal carcinoma revealed a subset of tumors harboring *NCOA4-RET* and novel *TRIM27-RET* fusions: a report of 17 cases. *Am J Surg Pathol*. 2018;42:1445–1455.
42. Weinreb I, Zhang L, Tirunagari LM, et al. Novel *PRKD* gene rearrangements and variant fusions in cribriform adenocarcinoma of salivary gland origin. *Genes Chromosomes Cancer*. 2014;53:845–856.
43. Antonescu CR, Katabi N, Zhang L, et al. *EWSR1-ATF1* fusion is a novel and consistent finding in hyalinizing clear-cell carcinoma of salivary gland. *Genes Chromosomes Cancer*. 2011;50:559–570.
44. Seethala RR, Dacic S, Cieply K, et al. A reappraisal of the *MECT1/MAML2* translocation in salivary mucoepidermoid carcinomas. *Am J Surg Pathol*. 2010;34:1106–1121.
45. Jee KJ, Persson M, Heikinheimo K, et al. Genomic profiles and *CRTC1-MAML2* fusion distinguish different subtypes of mucoepidermoid carcinoma. *Mod Pathol*. 2013;26:213–222.
46. Brill LB II, Kanner WA, Fehr A, et al. Analysis of *MYB* expression and *MYB-NFIB* gene fusions in adenoid cystic carcinoma and other salivary neoplasms. *Mod Pathol*. 2011;24:1169–1176.
47. Na K, Hernandez-Prera JC, Lim JY, et al. Characterization of novel genetic alterations in salivary gland secretory carcinoma. *Mod Pathol*. 2020;33:541–550.
48. Kastnerova L, Luzar B, Goto K, et al. Secretory carcinoma of the skin report of 6 cases, including a case with a novel *NFIX-PKN1* translocation. *Am J Surg Pathol*. 2019;43:1092–1098.
49. Satelli A, Li S. Vimentin in cancer and its potential as a molecular target for cancer therapy. *Cell Mol Life Sci*. 2011;68:3033–3046.
50. Kato S, Subbiah V, Marchlik E, et al. RET aberrations in diverse cancers: next-generation sequencing of 4871 patients. *Clin Cancer Res*. 2017;23:1988–1997.
51. Huang SC, Zhang L, Sung YS, et al. Frequent FOS gene rearrangements in epithelioid hemangioma: a molecular study of 58 cases with morphologic reappraisal. *Am J Surg Pathol*. 2015;39:1313–1321.
52. Ma Y, Miao Y, Peng Z, et al. Identification of mutations, gene expression changes and fusion transcripts by whole transcriptome RNAseq in docetaxel resistant prostate cancer cells [published correction appears in Springerplus. 2016 Dec 8;5(1):2084]. *Springerplus*. 2016;5:1861.
53. Stenman G, Andersson MK, Andren Y. New tricks from an old oncogene: gene fusion and copy number alterations of *MYB* in human cancer. *Cell Cycle*. 2010;9:2986–2995.